Inorganic Chemistry

including bioinorganic chemistry

November 17, 2014
Volume 53, Number 22
pubs.acs.org/IC

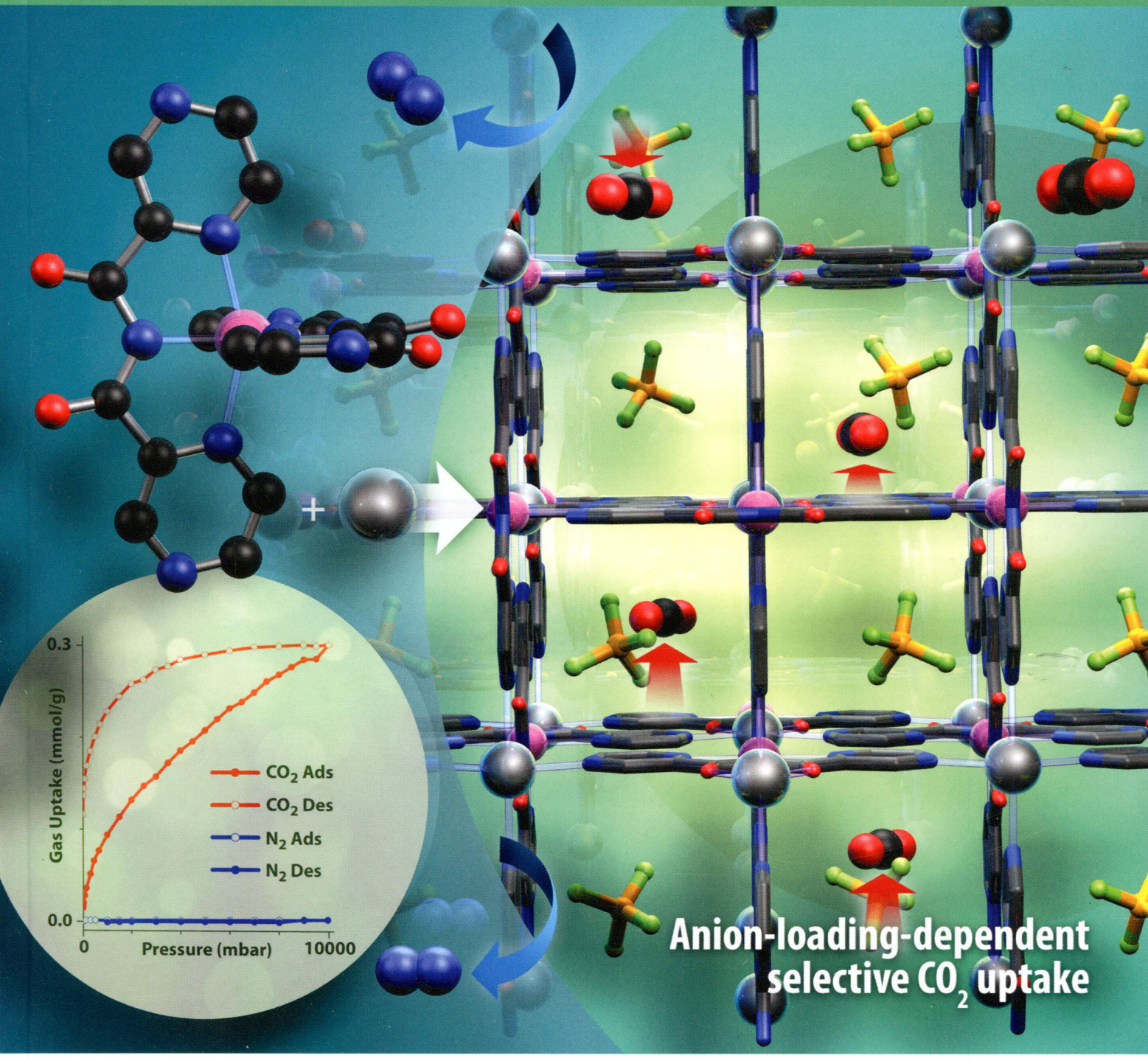

ACS Publications
Most Trusted. Most Cited. Most Read.

www.acs.org

Inorganic Chemistry

NOVEMBER 17, 2014
VOLUME 53 ISSUE 22

INOCAJ 53(22) 11809−12224 (2014)
ISSN 0020-1669
Registered in the U.S. Patent and Trademark Office

ON THE COVER: Doubling the anion occupancy in the channels of the metal organic framework (Ni^{II}-based MOF → Co^{III}-based MOF) increases the observed adsorption selectivity for CO_2 over N_2. These robust isostructural MOFs were assembled using $AgBF_4$ to activate the secondary coordination instructions present in the carefully designed monometallic pyrazine imide complexes of nickel(II) and cobalt(II or III). Cover created by Michael Crawford (Dunedin) from a concept provided by Sally Brooker. See M. G. Cowan, R. G. Miller, P. D. Southon, J. R. Price, O. Yazaydin, J. R. Lane, C. J. Kepert, and S. Brooker, p 12076.

Communications

11809 Ⓢ

DOI: 10.1021/ic501520c

Single-Molecule-Magnet Behavior in Mononuclear Homoleptic Tetrahedral Uranium(III) Complexes

Laura C. J. Pereira, Clément Camp, Joana T. Coutinho, Lucile Chatelain, Pascale Maldivi, Manuel Almeida,* and Marinella Mazzanti*

Two uranium coordination compounds, $[K(18c6)][U(OSi(O^tBu)_3)_4]$ and $[K(18c6)][U(N(SiMe_3)_2)_4]$, both presenting the U^{III} ion in similar pseudotetrahedral coordination environments but with different O- or N-donor ligands, show single-molecule-magnet behavior with similar energy barriers at ~24 K.

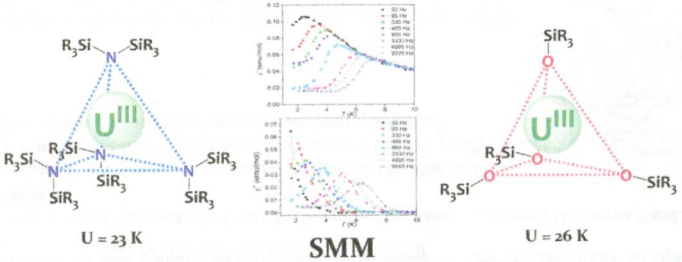

11812 Ⓢ

DOI: 10.1021/ic502325r

Hydroxo Radicals, C−H Activation, and Pt−C Bond Formation from 77 K Photolysis of a Platinum(IV) Hydroxo Complex

Lasantha A. Wickramasinghe and Paul R. Sharp*

Freezing a platinum(IV) hydroxo complex in a matrix switches the photochemistry from HOCl reductive elimination to hydroxo radical abstraction of a hydrogen atom from a phosphine ligand. Radical coupling of platinum(III) and carbon then forms a platinacycle, in which reductive eliminates a C−Cl bond.

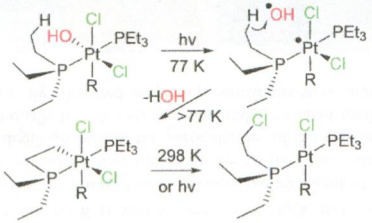

Award Paper

11815 DOI: 10.1021/ic502231m

N-Heterocyclic Carbene—Main-Group Chemistry: A Rapidly Evolving Field
Yuzhong Wang and Gregory H. Robinson*

This Award Article draws focus to our recent advances of the application of N-heterocyclic carbenes in stabilizing highly reactive main-group molecules. Syntheses, structures, computations, and reactivity studies of a host of interesting main-group compounds are presented. In an effort to provide historical context, our foundational work concerning the organogallium chemistry of sterically demanding *m*-terphenyl ligands is also discussed.

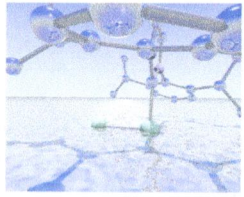

Articles

11833 (S) DOI: 10.1021/ic501990p

First-Principles Screening of Complex Transition Metal Hydrides for High Temperature Applications
Kelly M. Nicholson and David S. Sholl*

Semiautomated density functional theory and grand canonical linear programming (GCLP) methods are used to screen a library of 102 known complex transition metal hydrides to identify 13 materials with both enhanced stability relative to the associated binary hydrides and high operating temperature, $T > 1000$ K, for high temperature metal hydride applications. Thermodynamic properties and phase diagrams are predicted.

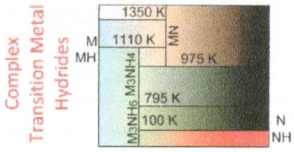

11849 (S) DOI: 10.1021/ic501992x

First-Principles Prediction of New Complex Transition Metal Hydrides for High Temperature Applications
Kelly M. Nicholson and David S. Sholl*

Semiautomated density functional theory and grand canonical linear programming methods are used to screen a library of 149 proposed complex transition metal hydrides to identify 81 thermodynamically viable materials at two levels of theory. Seven materials are identified with both enhanced stability relative to the associated binary hydrides and high operating temperature, $T > 1000$ K, for high temperature metal hydride applications. Thermodynamic properties and phase diagrams are predicted.

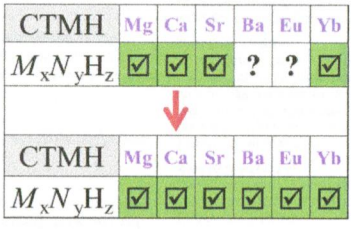

11861 DOI: 10.1021/ic4031156

A Dissociative Quantum Mechanical/Molecular Mechanical Molecular Dynamics Simulation and Infrared Experiments Reveal Characteristics of the Strongly Hydrolytic Arsenic(III)

Lorenz R. Canaval, Oliver M. D. Lutz, Alexander K. H. Weiss, Christian W. Huck, and Thomas S. Hofer*

The fate of the strongly hydrolytic arsenic(III) ion in water is investigated by means of a novel correlated quantum mechanical simulation involving a dissociative water model. Three hydrolysis events have been observed, and the sub-femtoseconds time scale of the simulation enabled an in-depth analysis of the particularities of the reaction intermediates. The final product has been characterized not only computationally but also via experimental attenuated total reflectance Fourier transform infrared spectroscopy. Furthermore, anharmonically corrected frequency evaluations were shown to complement the conclusions drawn.

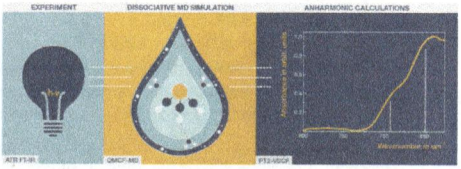

11871 DOI: 10.1021/ic502283d

"Spider"-Shaped Porphyrins with Conjugated Pyridyl Anchoring Groups as Efficient Sensitizers for Dye-Sensitized Solar Cells

Christina Stangel, Anthi Bagaki, Panagiotis A. Angaridis, Georgios Charalambidis, Ganesh D. Sharma,* and Athanasios G. Coutsolelos*

Two novel "spider-shaped" porphyrins, *meso*-tetraaryl-substituted **1PV-Por** and zinc-metalated **1PV-Zn-Por**, bearing four oligo(*p*-phenylenevinylene) (oPPV) pyridyl groups with long dodecyloxy chains on the phenyl groups, have been synthesized.

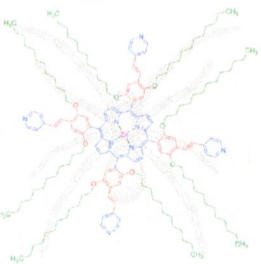

11882 DOI: 10.1021/ic501032t

Tuning the Emission Lifetime in Bis-cyclometalated Iridium(III) Complexes Bearing Iminopyrene Ligands

Ashlee J. Howarth, David L. Davies, Francesco Lelj, Michael O. Wolf,* and Brian O. Patrick

Bis-cyclometalated Ir(III) complexes with pyrene-containing ancillary ligands are reported. Synthetic modification of the pyrene-based ligand drastically effects the emission lifetimes observed. Extended emission lifetimes in these complexes compared to model complexes result from the triplet reservoir effect or the observation of dual emission with a long-lived pyrene (^{3}LC) component.

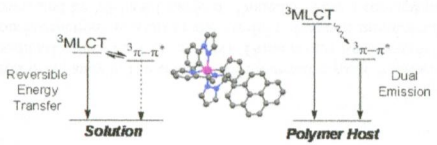

11890 S DOI: 10.1021/ic501049z

Activation Barriers of Oxygen Transformation at the Active Site of [FeFe] Hydrogenases

Arndt R. Finkelmann, Martin T. Stiebritz, and Markus Reiher*

A detailed mechanism of possible oxygen activation reactions at the active site of [FeFe] hydrogenases is discussed based on density functional theory calculations of reaction barriers.

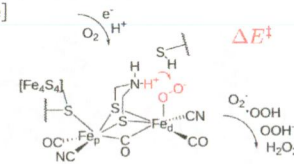

11903 S DOI: 10.1021/ic501084a

Solvolysis Mechanisms of RNA Phosphodiester Analogues Promoted by Mononuclear Zinc(II) Complexes: Mechanisic Determination upon Solvent Medium and Ligand Effects

Xuepeng Zhang, Yajie Zhu, Hui Gao, and Cunyuan Zhao*

Herein, we report a theoretical work of the mechanismic investigation on the cyclization of the RNA dinucleotide analogue 2-(hydroxypropyl)-4-nitrophenyl phosphate promoted by mononuclear zinc(II) complexes. The mechanistic preference on the ligand and solvent medium effects is discussed. The increasing size catalyst Zn:[12]aneN$_3$ provides a lower energy barrier and a significant mechanistic preference to the SBC mechanism. The reduced polarity solvents, such as methanol and ethanol, are more preferable for the catalytic reactions.

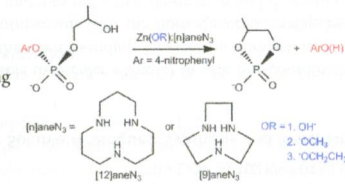

11913 S DOI: 10.1021/ic5010837

Comparison of the Active-Site Design of Molybdenum Oxo-Transfer Enzymes by Quantum Mechanical Calculations

Jilai Li and Ulf Ryde*

We have studied why the three families of molybdenum oxygen atom transfer enzymes have different active sites by quantum mechanical cluster calculations. The sites have different oxidative power, selected to give a reaction free energy close to zero, making the reoxidation or rereduction favorable. All active sites can reduce DMSO and oxidize sulfite (if Coulombic repulsion can be overcome), but only the xanthine oxidase model can oxidize xanthine, owing to the sulfido ligand.

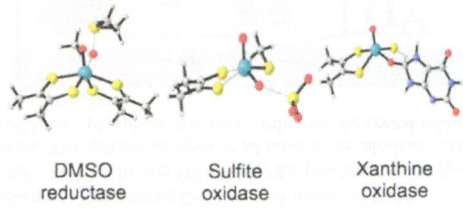

11925 S DOI: 10.1021/ic5011677

Axial Thiophenolate Coordination on Diiron(III)bisporphyrin: Influence of Heme–Heme Interactions on Structure, Function and Electrochemical Properties of the Individual Heme Center

Debangsu Sil, Firoz Shah Tuglak Khan, and Sankar Prasad Rath*

Syntheses, structures, and properties of a series of diiron(III)bisporphyrins with axial thiophenolate coordination have been reported. The large difference in chemical and electrochemical properties of the diheme as compared to the monoheme analog provides unequivocal evidence of the role played by interheme interactions.

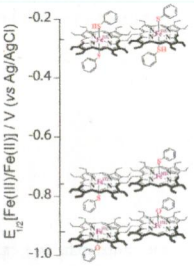

11937 S DOI: 10.1021/ic501342c

Influence of Calcium(II) and Chloride on the Oxidative Reactivity of a Manganese(II) Complex of a Cross-Bridged Cyclen Ligand

Zhan Zhang, Katherine L. Coats, Zhuqi Chen, Timothy J. Hubin,* and Guochuan Yin*

This work presents how Ca^{2+} and Cl^- affect the oxidation activity and redox potentials of the manganese complex of a cross-bridged cyclen ligand. Both Ca^{2+} and Cl^- can affect the redox potentials of the manganese complex, thus modulating its activity in oxidations. Adding Ca^{2+} to the manganese(II) and corresponding manganese(IV) complexes improves their catalytic activity in sulfide oxidation, while adding Cl^- to the manganese(IV) complex, which has no chloride ligand, greatly decreases its catalytic activity.

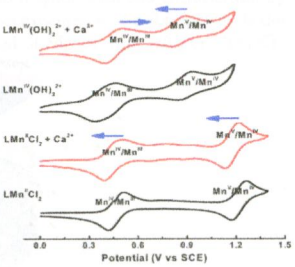

11948 S DOI: 10.1021/ic5014329

Six-Coordinate Nitrito and Nitrato Complexes of Manganese Porphyrin

T. S. Kurtikyan,* V. A. Hayrapetyan, M. M. Mehrabyan, and P. C. Ford*

Reaction of small increments of NO_2 gas with sublimed amorphous layers of $Mn^{II}(TPP)$ (TPP = *meso*-tetraphenylporphyrinato dianion) in a cryostat leads to formation of the 5-coordinate nitrato complex $Mn^{III}(TPP)(\eta^1\text{-}ONO_2)$ (**II**) through the two distinct steps with initial formation of the nitrito complex $Mn^{III}(TPP)(\eta^1\text{-}ONO)$ (**I**). Low-temperature interaction of **I** and **II** with the vapors of various ligands L leads to formation of the 6-coordinate nitrito $Mn^{III}(TPP)(L)(\eta^1\text{-}ONO)$ and nitrato $Mn^{III}(TPP)(L)(\eta^1\text{-}ONO_2)$ complexes (L = O-, S-, and N-donors).

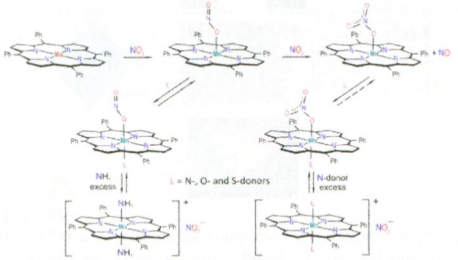

11960 S

DOI: 10.1021/ic501551y

Linear Coordination Fullerene C_{60} Polymer $[\{Ni(Me_3P)_2\}(\mu\text{-}\eta^2,\eta^2\text{-}C_{60})]_\infty$ Bridged by Zerovalent Nickel Atoms

Dmitri V. Konarev,* Salavat S. Khasanov, Yoshiaki Nakano, Akihiro Otsuka, Hideki Yamochi, Gunzi Saito, and Rimma N. Lyubovskaya

Coordination polymer $[\{Ni(Me_3P)_2\}(\mu\text{-}\eta^2,\eta^2\text{-}C_{60})]_\infty$ containing neutral fullerenes and zerovalent nickel atoms as bridges was obtained. Each nickel atom is linked in the polymer with two fullerene units by η^2-type bonds, providing a close approach of fullerenes to each other with a 9.693(3) Å interfullerene center-to-center distance.

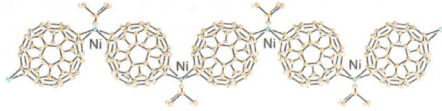

11966

DOI: 10.1021/ic5015576

Blue-Emitting Eu^{2+}-Activated LaOX (X = Cl, Br, and I) Materials: Crystal Field Effect

Donghyeon Kim, Sangha Park, Sungyun Kim,* Seong-Gu Kang, and Jung-Chul Park*

The emission spectra of LaOX:Eu^{2+} (X = Cl, Br, and I) show that the peak maxima change somewhat to the red-shift region: 425, 427, and 431 nm, respectively. The splitting energies of 5d orbitals are calculated; ΔE_{Cl} = 14 597 cm^{-1}, ΔE_{Br} = 14 864 cm^{-1}, ΔE_I = 15 001 cm^{-1} for LaOX:Eu^{2+} phosphors. It is noteworthy that the crystal field strength is dependent on the ionic radius of halide ions in LaOX:Eu^{2+} phosphors.

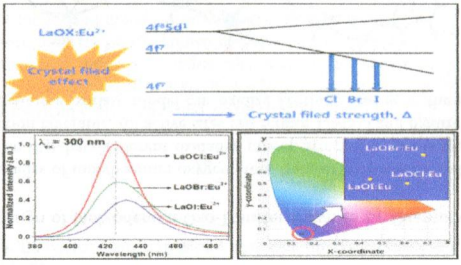

11974 S

DOI: 10.1021/ic501593k

Silica-Grafted 16-Electron Hydride Pincer Complexes of Iridium(III) and Their Soluble Analogues: Synthesis and Reactivity with CO

Martino Rimoldi and Antonio Mezzetti*

Iridium pincer complexes react with the surface silanols of SBA-15 (or with soluble molecular silanols) to give five-coordinate silica-grafted complexes of iridium(III), which react with carbon monoxide to the corresponding 18-electron adducts, as indicated by IR spectroscopy and solid-state ^{31}P and ^1H MAS NMR and by comparison with the homogeneous analogues. The Ir(III) PCP carbonyl complexes are stable, whereas the POCOP analogues undergo reductive elimination and degrafting.

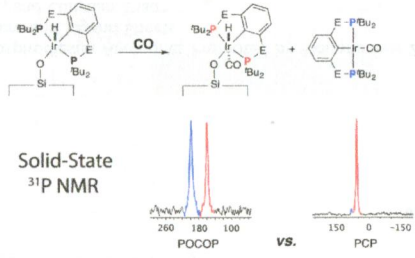

11985 DOI: 10.1021/ic501641q

A Novel Efficient Mn^{4+} Activated $Ca_{14}Al_{10}Zn_6O_{35}$ Phosphor: Application in Red-Emitting and White LEDs

Wei Lü,* Wenzhen Lv, Qi Zhao, Mengmeng Jiao, Baiqi Shao, and Hongpeng You*

Novel highly efficient deep red-emitting $Ca_{14}Al_{10}Zn_6O_{35}:Mn^{4+}$ phosphors were synthesized for blue-pumped light-emitting diodes. A red light and warm white light were created by combining the synthesized $Ca_{14}Al_{10}Zn_6O_{35}:Mn^{4+}$ phosphors with YAG:Ce and the blue InGaN LED chip.

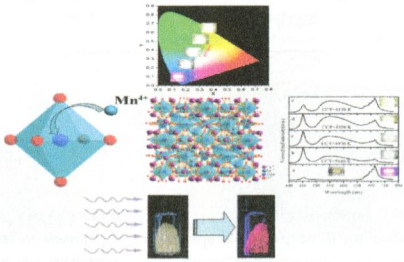

11991 DOI: 10.1021/ic501655u

Structural and Magnetic Diversity Based on Different Imidazolate Linkers in Cu(II)-Azido Coordination Compounds

Anindita Chakraborty, Srinivasa Rao Lingampalli, Aman Kumari, Joan Ribas, Jordi Ribas-Arino, and Tapas Kumar Maji*

Four magnetic Cu(II)-azido coordination compounds with diverse structural motifs were furnished by changing the substitution on the imidazole ring.

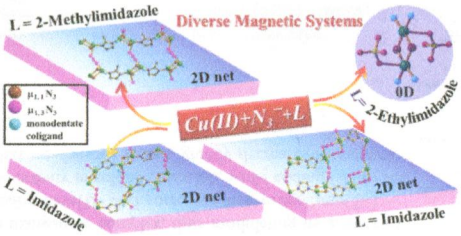

12002 DOI: 10.1021/ic501656s

Ligand-Centered Redox in Nickel(II) Complexes of 2-(Arylazo)pyridine and Isolation of 2-Pyridyl-Substituted Triaryl Hydrazines via Catalytic N-Arylation of Azo-Function

Debabrata Sengupta, Pradip Ghosh, Tanmay Chatterjee, Harashit Datta, Nanda D. Paul, and Sreebrata Goswami*

An experimental demonstration and analysis over redox noninnocent behavior of a series of Ni(II) complexes of 2-(arylazo)pyridine ligand have been presented. Development of an efficient method of Ni(II)-catalyzed synthesis of 2-pyridyl-substituted triaryl hydrazines is described, and this constitutes a major outcome of the present work. The hydrazines are strongly fluorescent dyes with multifaceted application possibilities.

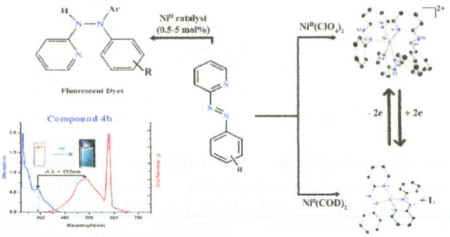

12014 S DOI: 10.1021/ic5016803

One-Dimensional and Two-Dimensional Anilate-Based Magnets with Inserted Spin-Crossover Complexes

Alexandre Abhervé, Miguel Clemente-León,* Eugenio Coronado,* Carlos J. Gómez-García, and Martin Verneret

The use of $[Fe^{III}(sal_2\text{-trien})]^+$ complexes and derivatives to prepare anionic anilate-based networks results in four two-dimensional compounds that show a ferrimagnetic ordering at ca. 10 K, whereas the inserted Fe(III) cations remain in the high- or low-spin state. $[Fe^{II}(tren(imid)_3)]^{2+}$ gives rise to a one-dimensional anilate-based compound with spin crossover of half of the Fe(II) complexes and ferromagnetic ordering below 2.5 K.

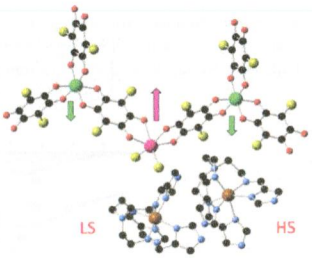

12027 S DOI: 10.1021/ic501736r

Formation Principles for Vanadium Selenites: The Role of pH on Product Composition

Jacob H. Olshansky, Karina J. Wiener, Matthew D. Smith, Anahita Nourmahnad, Max J. Charles, Matthias Zeller, Joshua Schrier, and Alexander J. Norquist*

Selection between the three compounds found in the $VOSO_4/SeO_2$/2-methylpiperazine system, $[C_5H_{14}N_2]$-$[(VO)_3(SeO_3)_2(HSeO_3)_4]$, $[C_5H_{14}N_2][VO(SeO_3)(HSeO_3)]_2{\cdot}2H_2O$ and $[C_5H_{14}N_2][VO(SeO_3)_2]$, can be achieved through adjustment of the initial reaction pH, which dictates the protonation state of selenous acid in solution. In addition, partial resolution of racemic 2-methylpiperazine in $[C_5H_{14}N_2][(VO)_3(SeO_3)_2(HSeO_3)_4]$ can be understood using a one-dimensional Ising model in which differences in hydrogen-bonding interactions account for a weakly correlated system.

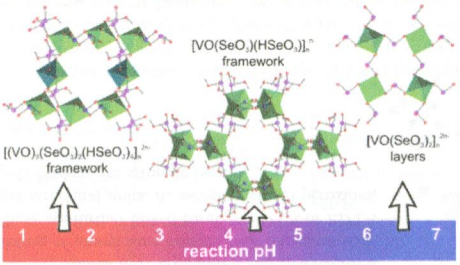

12036 S DOI: 10.1021/ic501741r

Multichromophoric Bimetallic Ru(II) Terpyridine Complexes Based on Pyrenyl-bis-phenylimidazole Spacer: Synthesis, Photophysics, Spectroelectrochemistry, and TD-DFT Calculations

Srikanta Karmakar, Dinesh Maity, Sourav Mardanya, and Sujoy Baitalik*

Bimetallic Ru(II)-terpyridine complexes based on pyrenyl-bis-phenylimidazole spacer show room-temperature emission with reasonably long excited-state lifetimes and exhibit IVCT band in the NIR region despite the fact that the two ruthenium atoms are separated by about 30 Å.

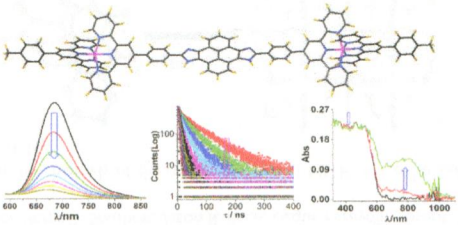

12050 S DOI: 10.1021/ic5017593

Alkaline Earth Metal (Mg, Sr, Ba)–Organic Frameworks Based on 2,2′,6,6′-Tetracarboxybiphenyl for Proton Conduction
Xi-Yan Dong, Xiao-Peng Hu, Hong-Chang Yao, Shuang-Quan Zang,* Hong-Wei Hou, and Thomas C.W. Mak

Three new alkaline earth metal (Mg, Sr, Ba) based metal–organic frameworks have been synthesized by using 2,2′,6,6′-tetracarboxybiphenyl as linker. Novel water aggregates are incorporated in these MOFs, which exhibit interesting structural diversity, variable chemical and thermal stability, as well as proton conduction.

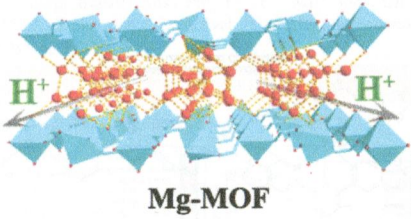

12058 S DOI: 10.1021/ic501776h

Investigation of New Alkali Bismuth Oxosulfates and Oxophosphates with Original Topologies of Oxo-Centered Units
Minfeng Lü, Marie Colmont,* Marielle Huvé, Isabelle De Waele, Christine Terryn, Almaz Aliev, and Olivier Mentré*

The first alkali bismuth oxosulfates, $[Bi_{12}O_{15}]Li_2(SO_4)_4$ and $[Bi_7K_2O_8]K(SO_4)_4$, have been synthesized and characterized by single crystal XRD, transmission electron microscopy, and multiphoton SHG and IR spectroscopy. In the above formula the $[Bi_xO_y]$ subunits denote the 3D-porous or 1D-columnar polycationic host-lattice formed of edge-sharing OBi_4 or $O(Bi,K)_4$ oxocenterd tetrahedral into novel topologies.

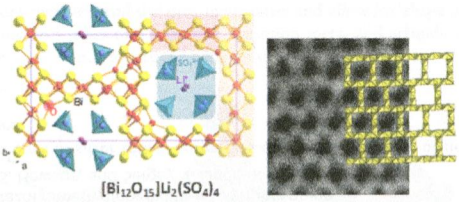

12066 S DOI: 10.1021/ic501816v

To Bend or Not To Bend: Experimental and Computational Studies of Structural Preference in $Ln(Tp^{iPr_2})_2$ (Ln = Sm, Tm)
Aurélien Momin, Lee Carter, Yi Yang, Robert McDonald, Stéphanie Essafi (née Labouille), François Nief, Iker Del Rosal, Andrea Sella,* Laurent Maron,* and Josef Takats*

Contrary to the simple ^1H NMR spectra, implying symmetrical solution structure, the solid-state structures of $Ln(Tp^{iPr2})_2$ (Ln = Sm, Tm) revealed an unexpected bent-sandwich-like geometry. DFT calculations revealed that the bent geometry is the result of a felicitous combination of steric congestion and secondary $^iPrC–H\cdots N$ H-bonding interactions. The importance of these secondary interactions is discussed in relation to MX_2 (M = Gp II and Ln(II), X = halide and η-C_5R_5) compounds.

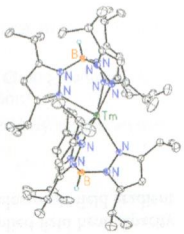

12076 S

DOI: 10.1021/ic501876m

Selective Gas Adsorption in a Pair of Robust Isostructural MOFs Differing in Framework Charge and Anion Loading

Matthew G. Cowan, Reece G. Miller, Peter D. Southon, Jason R. Price, Ozgur Yazaydin, Joseph R. Lane, Cameron J. Kepert,* and Sally Brooker*

Doubling the anion occupancy in the channels of the MOF (Ni^{II}-based MOF → Co^{III}-based MOF) increases the observed adsorption selectivity for CO_2 over N_2.

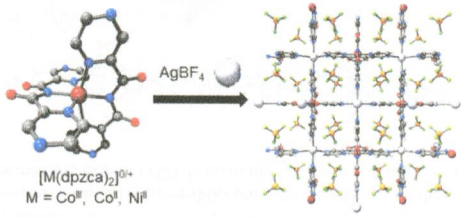

12084 S

DOI: 10.1021/ic5018906

Expanding the Crystal Chemistry of Uranyl Peroxides: Four Hybrid Uranyl-Peroxide Structures Containing EDTA

Jie Qiu, Jie Ling, Claire Sieradzki, Kevin Nguyen, Ernest M. Wylie, Jennifer E. S. Szymanowski, and Peter C. Burns*

Four uranyl peroxides containing EDTA ligands were crystallized and characterized that contain structural units consisting of uranyl ions bridged into tetramers and dimers through peroxo groups. These are further linked through EDTA or EDTA oxidized by peroxide to form larger structural units. As in other uranyl peroxides, the dihedral angles of the U–O_2–U bridges are strongly bent.

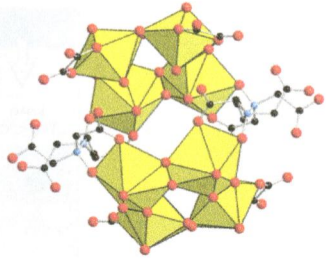

12092 S

DOI: 10.1021/ic501915j

Single-Molecule Magnet Behavior and Magnetocaloric Effect in Ferromagnetically Coupled Ln^{III}-Ni^{II}-Ni^{II}-Ln^{III} (Ln^{III} = Dy^{III} and Gd^{III}) Linear Complexes

Carlos Meseguer, Silvia Titos-Padilla, Mikko M. Hänninen, R. Navarrete, A. J. Mota, Marco Evangelisti, José Ruiz, and Enrique Colacio*

New types of linear tetranuclear Ln^{III}–Ni^{II}–Ni^{II}–Ln^{III} (Ln^{III} = Dy **1**, Gd **2**) complexes with alternating Gd(μ-diphenoxo)Ni and Ni(μ-bisphenylenediimine)Ni bridging fragments have been structurally and magnetically characterized. The Dy_2Ni_2 complex exhibits single-molecule magnet behavior, whereas the isostructural Gd_2Ni_2 presents significant magneto-caloric effect. The reduction of the MCE effect promoted by the Ni^{II} magnetic anisotropy has been quantified to be of approximately a six percent.

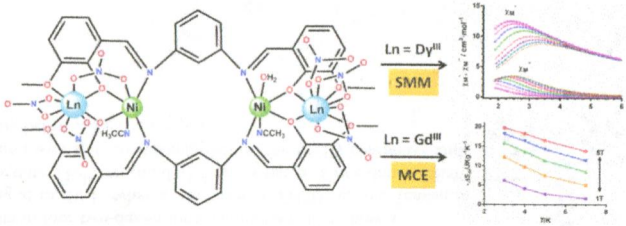

12100 S

DOI: 10.1021/ic501925e

Measurement of Extreme Hyperfine Fields in Two-Coordinate High-Spin Fe^{2+} Complexes by Mössbauer Spectroscopy: Essentially Free-Ion Magnetism in the Solid State

Aimee M. Bryan, Chun-Yi Lin, Michio Sorai,* Yuji Miyazaki, Helen M. Hoyt, Annelise Hablutzel, Anne LaPointe, William M. Reiff,* Philip P. Power,* and Charles E. Schulz*

Zero- and applied-field Mössbauer spectroscopy for three linearly coordinated high-spin Fe^{2+} derivatives, namely, $Fe\{N(SiMe_3)Dipp\}_2$ (**1**) (Dipp = C_6H_3-2,6-^{i}Pr$_2$), $Fe(OAr')_2$ (**2**) [Ar' = C_6H_3-2,6-$(C_6H_3$-2,6-^{i}Pr$_2)_2$], and $Fe\{C(SiMe_3)_3\}_2$ (**3**), show that they have very high internal magnetic fields, with the field of 162 T (where the measured 171 T effective field includes the 9 T applied field) for **1** representing the highest known for any iron species. Zero- and applied-field heat-capacity measurements on **3** establish a g_{eff} value near 12, consistent with the principal component of the ligand electronic field gradient being coincident with the z axis.

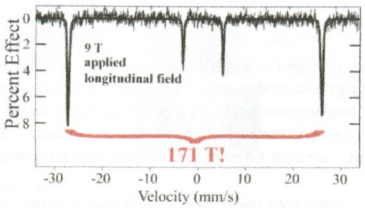

12108 S

DOI: 10.1021/ic5019357

Isomer Dependence in the Assembly and Lability of Silver(I) Trifluoromethanesulfonate Complexes of the Heteroditopic Ligands, 2-, 3-, and 4-[Di(1*H*-pyrazolyl)methyl]phenyl(di-*p*-tolyl)phosphine

James R. Gardinier,* Jeewantha S. Hewage, and Sergey V. Lindeman

The solid state and solution structures of silver triflate complexes of the three isomers of new P,N–N heteroditopic ligands are examined.

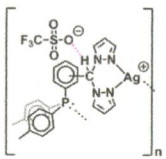

12122 S

DOI: 10.1021/ic501946f

Three Steps in One Pot: Synthesis of Linear Bilateral Extended 2,2′:6′,2″-Terpyridineruthenium(II) Complexes

Janis Veliks, Olivier Blacque, and Jay S. Siegel*

A new one-pot reaction has been developed to obtain linear bilateral extended 2,2′:6′,2″-terpyridineruthenium(II) complexes via in situ cleavage of the methoxymethyl (MOM) protecting group, cycloisomerization, and metal complexation of 5,5″-bis(methoxymethoxy)-4,4″-bis(substituted ethynyl)-2,2′:6′,2″-terpyridines in the presence of $Ru(DMSO)_4Cl_2$.

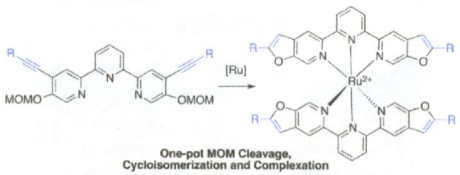

12127 Ⓢ DOI: 10.1021/ic501978u

Anion-Directed Assemblies of Cationic Metal–Organic Frameworks Based on 4,4′-Bis(1,2,4-triazole): Syntheses, Structures, Luminescent and Anion Exchange Properties

Xinxiong Li, Yaqiong Gong, Huaixia Zhao, and Ruihu Wang*

Three 3-D cationic MOFs based on 4,4′-bis(1,2,4-triazole) and Ag^+ were presented. The type, size, and shape of anions have important effects on bridging modes of btr and the cationic frameworks. The MOF containing a PF_6^- anion can selectively exchange MnO_4^- in aqueous solution with a modest capacity of 0.56 mol mol^{-1}; the luminescent emission is quickly quenched upon MnO_4^- exchange.

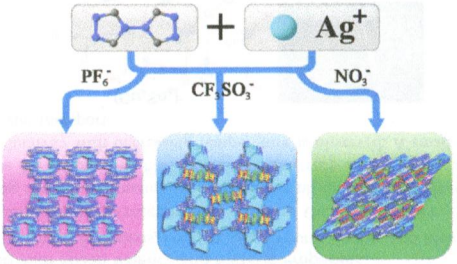

12135 Ⓢ DOI: 10.1021/ic501985p

Dissociation of Diglycolamide Complexes of Ln^{3+} (Ln = La–Lu) and An^{3+} (An = Pu, Am, Cm): Redox Chemistry of 4f and 5f Elements in the Gas Phase Parallels Solution Behavior

Yu Gong, Guoxin Tian, Linfeng Rao, and John K. Gibson*

Fragmentation of tripositive lanthanide and actinide gas-phase coordination complexes reveals f-element redox chemistry. Retention of the trivalent oxidation state is prevalent. The divalent oxidation state is dominant for Eu but minor for Yb and Sm. Only for Pu is the tetravalent oxidation state seen. The results reflect the III/II and IV/III reduction potentials: dissociation of multiply charged coordination complexes provides a probe of metal ion redox chemistry.

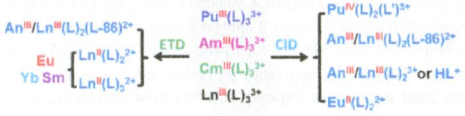

12141 DOI: 10.1021/ic502058r

Tunable-Color Luminescence via Energy Transfer in $NaCa_{13/18}Mg_{5/18}PO_4$:A (A = Eu^{2+}/Tb^{3+}/Mn^{2+}, Dy^{3+}) Phosphors for Solid State Lighting

Kai Li, Jian Fan, Xiaoyun Mi, Yang Zhang, Hongzhou Lian,* Mengmeng Shang, and Jun Lin*

A succession of $NaCa_{13/18}Mg_{5/18}PO_4$ (NCMPO):A (A = Eu^{2+}/Tb^{3+}/Mn^{2+}, Dy^{3+}) phosphors prepared by the high-temperature solid-state reaction method can be effectively excited under UV radiation, which show tunable color from purple-blue to red including white based on energy transfer from Eu^{2+} to Tb^{3+}/Mn^{2+} ions. Under low-voltage electron beam bombardment excitation, the NCMPO:A display their, respectively, characteristic emissions with different colors. It suggests their potential applications in WLEDs and FEDs.

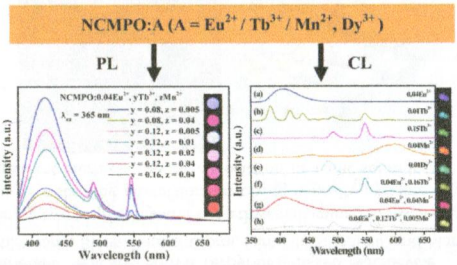

12151 DOI: 10.1021/ic5021077

Stereochemistry of Complexes with Double and Triple Metal–Ligand Bonds: A Continuous Shape Measures Analysis

Santiago Alvarez,* Babil Menjón, Andrés Falceto, David Casanova, and Pere Alemany

Normalized coordination polyhedra remove bond distance inequalities and allow for shape analyses of distortions associated with bond angles only. Applications to studies of a variety of transition metal and actinide complexes with metal–ligand multiple bonds disclose stereochemical trends associated with polyhedral interconversion or ligand association/dissociation paths.

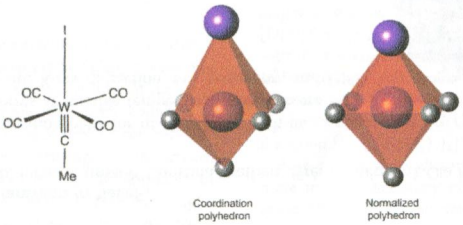

12164 DOI: 10.1021/ic502047q

Hydride Binding to the Active Site of [FeFe]-Hydrogenase

Petko Chernev, Camilla Lambertz, Annika Brünje, Nils Leidel, Kajsa G. V. Sigfridsson, Ramona Kositzki, Chung-Hung Hsieh, Shenglai Yao, Rafael Schiwon, Matthias Driess, Christian Limberg, Thomas Happe, and Michael Haumann*

Structures of H-cluster intermediates in [FeFe]-hydrogenase from X-ray spectroscopy and quantum chemistry suggest an iron-bound hydride in the super-reduced state.

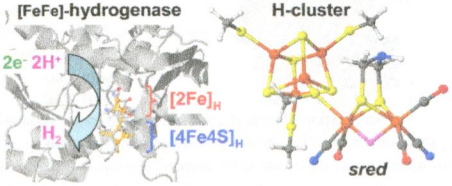

12178 DOI: 10.1021/ic502121k

Mixture of Fuels Approach for the Synthesis of $SrFeO_{3-\delta}$ Nanocatalyst and Its Impact on the Catalytic Reduction of Nitrobenzene

Akula Naveenkumar, Praveena Kuruva, Chikkadasappa Shivakumara, and Chilukoti Srilakshmi*

For the first time modified solution combustion synthesis approach was applied for the synthesis of $SrFeO_{3-\delta}$ nanocatalyst. Mixture of fuels synthesis approach prevents agglomeration of particles and leads combustion reaction will takes place at lower temperatures than the single fuels. Crystallite size of the $SrFeO_{3-\delta}$ material can be reduced to half that of the material obtained by single fuel. The present approach also impacted the activity of the catalysts for the reduction of nitrobenzene to azoxybenzene.

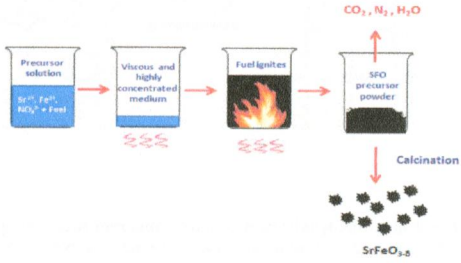

12186 DOI: 10.1021/ic502141q

Synergistic Coupling of Fluorescent "Turn-Off" with Spectral Overlap Modulated FRET for Ratiometric Ag^+ Sensor

Mengliang Zhu, Yabin Zhou, Liguo Yang, Lin Li, Dongdong Qi, Ming Bai, Yuting Chen, Hongwu Du,* and Yongzhong Bian*

Upon selective binding of Ag^+ to a BODIPY-porphyrin dyad (**1**), the synergistic coupling of a spectral overlap modulated FRET with a fluorescence quenching process leads to remarkable intensity ratio changes of two distinct emissions (F_{513}/F_{654}), which allow for the ratiometric detecting of Ag^+ with excellent sensitivity in solution and living cells.

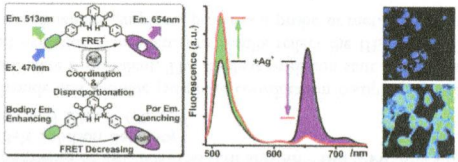

12191 DOI: 10.1021/ic502137m

$NaCu_6Se_4$: A Layered Compound with Mixed Valency and Metallic Properties

Mihai Sturza, Christos D. Malliakas, Daniel E. Bugaris, Fei Han, Duck Young Chung, and Mercouri G. Kanatzidis*

New 2D compound, $NaCu_6Se_4$, forms from the reaction of Na_2Se_x and Cu, and by direct combination reactions. We present detailed characterization including synthesis, structure, and properties of mixed valence $NaCu_6Se_4$, which has unique $[Cu_6Se_4]^-$ layers sandwiching the Na cations. We find that the conductivity of this compound is $\sim 3 \times 10^3$ S cm^{-1} at room temperature, and increasing conductivity with decreasing temperature is observed. A small positive thermopower and Hall effect measurements indicate p-type transport.

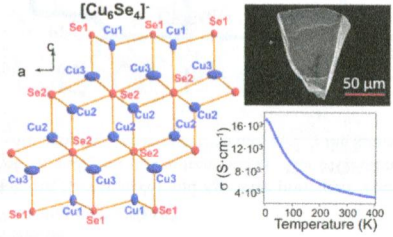

12199 Ⓢ DOI: 10.1021/ic501849g

Homochiral Metal–Organic Frameworks with Enantiopure Proline Units for the Catalytic Synthesis of β-Lactams

Zhong-Xuan Xu, Yan-Xi Tan, Hong-Ru Fu, Juan Liu, and Jian Zhang*

Two enantiopure organic ligands integrating flexible proline units and rigid isophthalate units have been rationally designed and employed for the construction of four homochiral porous metal–organic frameworks (MOFs), respectively. One pair of these MOFs are used as heterogeneous catalysts to construct β-lactam derivatives.

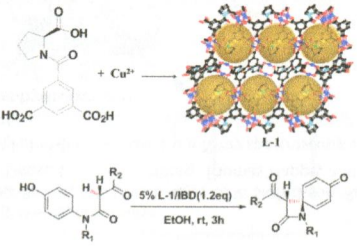

12205 Ⓢ DOI: 10.1021/ic502224y

Perovskite to Postperovskite Transition in $NaFeF_3$

Fabian L. Bernal, Kirill V. Yusenko, Jonas Sottmann, Christina Drathen, Jérémy Guignard, Ole Martin Løvvik, Wilson A. Crichton, and Serena Margadonna*

The structural, magnetic, and transition behavior of $NaFeF_3$ in both its perovskite and postperovskite forms at variable temperature and pressure conditions is described from in situ X-ray diffraction, magnetometry, and DFT calculations.

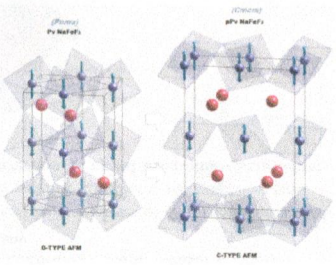

12215 Ⓢ DOI: 10.1021/ic502329s

Formation of Double-Strand Dimetallic Helicates with a Terpyridine-Based Macrocycle

Carla Bazzicalupi, Antonio Bianchi,* Tarita Biver, Claudia Giorgi, Samuele Santarelli, and Matteo Savastano

The macrocyclic ligand L, containing two terpyridine and two ethylenediamine groups, forms a double-strand helicate Cu_2L^{4+} complex stabilized by interstrand π–π stacking interactions involving opposite pyridine rings. The complex shows high thermodynamic stability and significant inertness toward dissociation in acidic solutions.

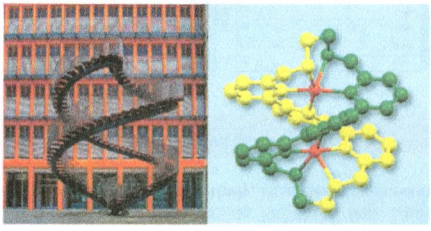

Ⓢ Supporting Information available via online article